Electronic Supplementary Information (ESI)

Pressure-induced water production using a copper–chromium Prussian blue analog

Shintaro Akagi,[§] Mayuko Tanaka,[§] Junhao Wang, Hisao Kiuchi, Yoshihisa Harada, Yizhou Chen, Kazuhiro Marumoto, Kenta Imoto, Shin-ichi Ohkoshi,* Hiroko Tokoro*

Table of Contents

Experimental Section

§1. Physical measurements.

Elemental analysis was performed by Agilent 7700x inductively coupled plasma mass spectroscopy (ICP-MS) for Cu and Cr and by standard microanalytical methods for C, H, and N. A uniaxial pressure pellet-forming machine was used to apply pressure to samples. The water expelled by compressing the sample with a uniaxial pellet machine for 10 min was separated and collected using a pipette. PXRD patterns were measured with a Rigaku Ultima IV using Cu Kα radiation. Rietveld analyses for the XRD patterns were performed by using Rigaku PDXL software. Dynamic vapour sorption (DVS) measurements were performed using an E-301 apparatus (East Core, Ltd.). The sample weight was calibrated at 26 °C and 27% RH. The morphologies of the samples were examined using scanning electron microscopy (SEM, JSM-7500FA, JEOL). Infrared (IR) spectra were recorded by a JASCO FT/IR-4700 spectrometer using CaF_2 plates as a sample holder. Liquid paraffin was used to hold powder samples on CaF_2 plates. Lines were extrapolated for the wavenumber region where the IR signal from the sample was not observed due to liquid paraffin (2750–3050 cm^{-1}). The IR spectra were used to estimate the number of water molecules before and after pressure application. To compare the intensity of the IR spectra of CuCr PBA before and after pressure application, the intensity of the IR spectra were calibrated as follows: SiO_2 powder, which has a peak around 900–1300 cm^{-1} unaffected by applying pressure and does not overlap with the peaks of CuCr PBA (Figure S3), was used as the standard material. From the spectra of the mixed sample of CuCr PBA and SiO_2 at 0.1, 0.5, 1 and 2 GPa, the ratio of the oscillator strength of the peak of Cu–NC–Cr (2180 cm^{-1}) to that of the peak of Cu–CN–Cr (2115 cm^{-1}) is estimated as 0.27, i.e., the intensity ratio of peak Cu–NC–Cr (2180 cm^{-1}) and Cu–CN–Cr (2115 cm^{-1}) is 1 : 3.7. This intensity ratio was used to calibrate the intensities of IR spectra of CuCr PBA before and after pressure application. IR spectra and XRD measurements were conducted at (25°C and 47% RH) and (24°C and 40% RH), respectively, which indicated that z = 7.4 before pressure application.

The valence states of Cu, Cr, and O on CuCr PBA samples were measured at SPring-8 BL07LSU in the form of pressed pellets. Humidity during the measurements was kept below 30% RH. To maintain a barrier between the vacuum and pressed pellet in the atmosphere, a sample cell was developed comprising a 150-nm-thick silicon carbide (SiC) membrane with a 11-nm-thick Au coat (NTT-AT Corp., Japan). To minimize absorption caused by the thin air layer between the SiC membrane and the pressed pellet, an Al rod was used to gently push the sample towards the SiC membrane from the backside. A pellet with a very weak uniaxial pressure of 7.5 x 10^{-2} GPa was used as a sample before pressure application. X-ray absorption spectra were collected in partial fluorescence mode by using a silicon drift detector (Amptek FAST SDD®) that extracts emission signals of the target element, which reduces background noise. X-ray emission spectra from the oxygen in H_2O were collected under non-resonant condition by 550 eV excitation. All X-ray spectroscopy measurements were conducted at ambient temperature. The intensity changes observed in XES and XAS spectra by applying pressure are relatively small compared to that of IR spectra. As the reason of these intensity changes, the following reasons are considered. One is that the sample before applying pressure actually experiences a pressure of 7.5 x 10^{-2} GPa to form a pellet (Figure S10). Due to this low-pressure application, it is possible that some water molecule is removed from CuCr PBA. The other possible reason is, since the IR measurements were carried out immediately after pressure release, while the XES measurements were performed after leaving the sample for several days under normal atmospheric conditions (it needed to be shipped to the Spring8 facility from the University of Tsukuba), which could have allowed some water molecules to re-enter the CuCr PBA.

Results and Discussion

§2. Crystallographic data of CuCr PBA.

Table S1a. Atomic positions of CuCr PBA under atmospheric pressure obtained by Rietveld refinement of the XRD pattern.

Atoms	*x/a*	*y/b*	*z/c*	Occupancy
Cu	0.500	0.500	0.500	1.000
Cr	0.500	0.500	0.000	0.667
C	0.500	0.500	0.187	0.667
N	0.500	0.500	0.293	0.667
O1	0.539	0.461	0.295	0.083
O2	0.750	0.250	0.250	0.667
O3	0.657	0.343	0.157	0.170

* Crystal system: Cubic ($Fm\bar{3}m$) with the lattice constant a = 10.3810(2) Å, R_w = 2.38, and S = 1.55.

** XRD measurements were conducted at 24°C and 40% RH, for which the composition had the formula $Cu_{1.5}[Cr(CN)_6]\cdot 7.0H_2O$.

Table S1b. Atomic positions of CuCr PBA after pressure application of 2 GPa obtained by Rietveld refinement of the XRD pattern.

Atoms	*x/a*	*y/b*	*z/c*	Occupancy
Cu	0.500	0.500	0.500	1.000
Cr	0.500	0.500	0.000	0.667
C	0.500	0.500	0.187	0.667
N	0.500	0.500	0.293	0.667
O1	0.539	0.461	0.295	0.083
O2	0.750	0.250	0.250	0.630
O3	0.657	0.343	0.157	0.000

*Crystal system: Cubic ($Fm\bar{3}m$) with the lattice constant a = 10.3776(6) Å, R_w = 1.56, and S = 1.08.

** XRD measurements were conducted at 24°C and 40% RH, for which the composition had the formula $Cu_{1.5}[Cr(CN)_6]\cdot 4.9H_2O$.

§3. Pressure-induced water production by CuCr PBA

Photographs from the water production experiment performed on CuCr PBA at 2 GPa are presented in Figure S1. When a pressure of 2 GPa was applied at 24°C and 57% RH, water droplets formed, similar to the behavior noted with the application of 1 GPa pressure (refer to Figure 2 in the main text). After applying 1 GPa, we successfully removed the mold from the press and examined the sample. However, after applying 2 GPa, the sample was compressed more tightly, making it impossible to remove the mold without disturbing the water droplets that had accumulated around the sample. Consequently, the photograph taken at 1 GPa, which more clearly illustrates the process of water emerging from the sample under pressure, was chosen as Figure 2 in the main text.

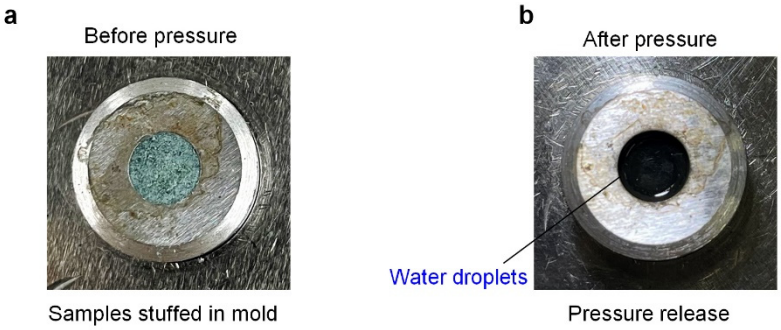

Figure S1. Pressure-induced water production by CuCr PBA. Powder samples were packed into molds (a). A uniaxial pressure of 2 GPa was applied to the sample (b). After the pressure was released, water was expelled from the sample. The photographs were taken from above the sample. Based on Figure S3, the estimated number of water molecules in the composition before pressure application at 24°C and 57% RH (56% RH for 1 GPa in Figure 2) was 7.9, resulting in a composition of $Cu_{1.5}[Cr(CN)_6]\cdot 7.9H_2O$.

§4. Time dependence of the expelled water mass under applied pressure.

The mass of water expelled by varying the pressure application time (1, 3, 5, 7, and 10 min) is shown in Figure S2. The mass of the expelled water increased as the pressure application time increased up to 3 min. However, for times longer than 3 min, the mass remained almost unchanged, indicating that a pressure application time of at least 3 min is necessary for water production. The pressure was applied for a total duration of 10 min for water collection.

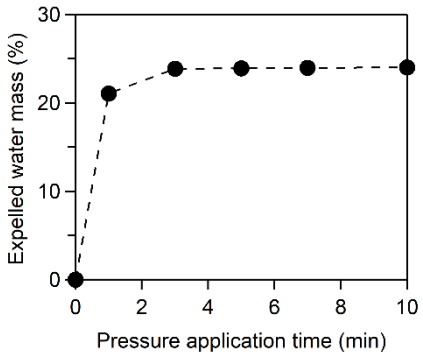

Figure S2. Time dependence of the mass of expelled water from CuCr PBA after applied pressure.

§5. Quality of the water produced by applying pressure.

The concentrations of Cu and Cr ions in the water that was formed by applying pressure were analysed using Perkin Elmer Plasma Mass Spectrometer ELAN DRC-e (ICP-MS). The results showed that the Cu content was 404 ppm (0.04 wt%) and the Cr ion content was 80 ppm (0.008 wt%). Based on these concentrations, the total weight of dissolved Cu, Cr, C, and N resulting from the application of pressure was estimated to be 0.2 mg per 1 g of CuCr PBA (0.02%), which is a small amount. To purify the water by removing these metal ions, Cu and Cr, it is necessary to select an appropriate method based on the removal objective and required removal concentration. Common methods for removing metal ions from water include precipitation/coprecipitation (chemical precipitation), ion exchange, adsorption, electrochemical methods, and membrane separation. The pH of the water obtained upon pressure application, as measured using a HORIBA LAQUAtwin pH meter, was found to be 3.6, indicating weak acidity. The results of three organic elemental analyses, performed using an Elementar UNICUBE elemental analyser, indicated that the water generated from the CuCr PBA contained almost no detectable C or N (Table S2). Considering that the estimated concentrations of C and N based on the ICP-MS results were within the range of 0.01–0.04 wt%, which is below the detection limit of the Elementar UNICUBE organic elemental analysis (±0.3 wt%), the absence of detectable C and N in the organic elemental analysis is a reasonable conclusion.

Table S2. Results of organic elemental analysis of water droplets released from CuCr PBA upon pressure application

	C (wt%)	N (wt%)
1	0.00	0.00
2	0.02	0.06
3	0.00	0.00

§6. Dependence of the water content on the humidity.

The water content (z) of CuCr PBA varies with humidity (Figure S3). Elemental analysis conducted at 26°C and 27% RH indicated that z = 6.4.

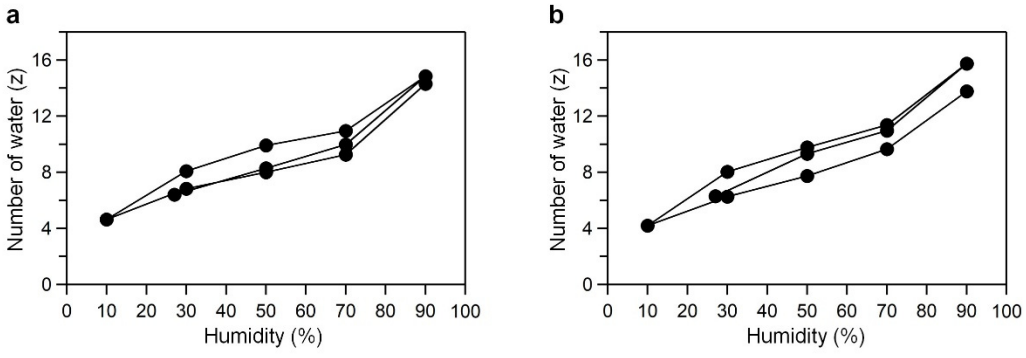

Figure S3. Dependence of the water content in the CuCr PBA sample on the humidity at (a) 26°C and (b) 30°C. Isotherm curves of CuCr PBA were collected in a nitrogen atmosphere at 10%–80% RH by using DVS equipment.

§7. Extrapolated curves for the IR spectra at 2750–3050 cm^{-1}.

Figure S4 shows the IR signals before and after pressure application as light gray and light red, respectively. The IR signals at 2750–3050 cm^{-1}, which corresponds to the region not detected from the sample due to liquid paraffin, were extrapolated, and they are shown as dotted lines. The extrapolated lines were used to estimate the areas of the IR peak from water. Based on the IR spectra, the compositions before and after pressure application at 25°C and 47% RH were estimated to have formulas of $Cu^{II}_{1.5}[Cr^{III}(CN)_6]_{0.71}[Cr^{III}(NC)_6]_{0.29}\cdot 7.4H_2O$ and $Cu^{II}_{1.5}[Cr^{III}(CN)_6]_{0.17}[Cr^{III}(NC)_6]_{0.83}\cdot 4.9H_2O$, respectively. The chemical formula of CuCr PBA in the text describes $Cu_{1.5}[Cr(CN)_6]\cdot zH_2O$ for clarity.

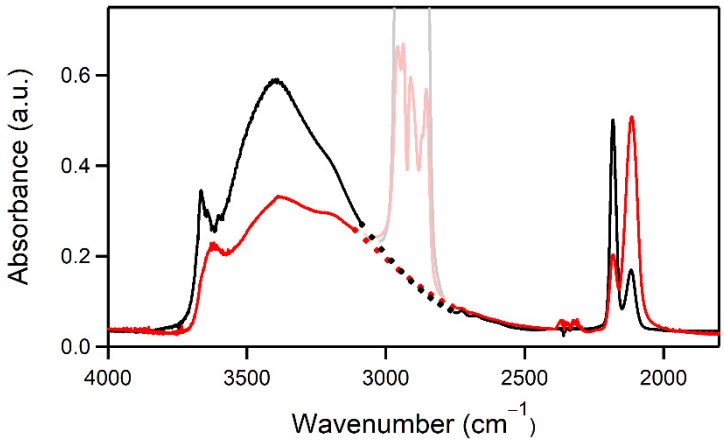

Figure S4. IR spectra at 25°C and 47% RH before (black) and after (red) pressure application of 2 GPa. The observed spectra are shown as solid lines, and the extrapolated spectra are shown as dotted lines.

§8. IR spectra of SiO_2 before and after pressure application.

Figure S5 presents the IR spectra of SiO_2, used as the reference standard, to normalize the IR spectra intensities of CuCr PBA both before and after the pressure application of 2GPa. The IR spectra of SiO_2 does not exhibit meaningful changes by the pressure application of 2 GPa.

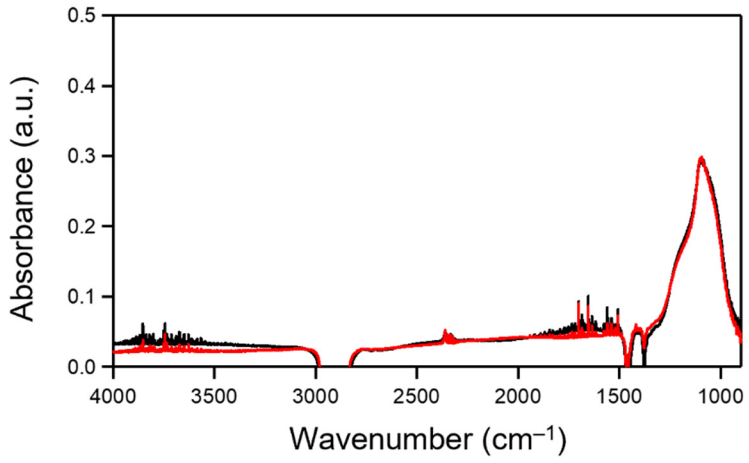

Figure S5. IR spectra of SiO_2 before (black line) and after (red line) pressure application of 2 GPa.

§9. Reference experiments on pressure-induced water production in various PBAs.

To verify whether pressure-induced water production was observed, we synthesised and investigated nine reference PBA samples with $Cr(CN)_6$ or $Co(CN)_6$ cyanide metal centers. The chemical compositions and elemental analysis (26°C, 27% RH) results of the synthesised samples are presented below: $Mn^{II}_{1.5}[Cr^{III}(CN)_6]\cdot 8.0H_2O$ (**MnCr**), Calculated: Mn, 18.96; Cr, 11.96; C, 16.58; N, 19.34; H, 3.71 %; Found: Mn, 18.67; Cr, 11.94; C, 17.23; N, 20.21; 3.44%. $Fe^{II}_{1.5}[Cr^{III}(CN)_6]\cdot 7.2H_2O$ (**FeCr**), Calculated: Fe, 19.87; Cr, 12.33; C, 17.09; N, 19.94; H, 3.44%; Found: Fe, 19.49; Cr, 12.65; C, 17.18; N, 20.10; H, 3.14 %. $Co^{II}_{1.5}[Cr^{III}(CN)_6]\cdot 8.3H_2O$ (**CoCr**), Calculated: Co, 19.82; Cr, 11.66; C, 16.15; N, 18.84; H, 3.75%; Found: Co, 19.88; Cr, 11.71; C, 15.98; N, 18.73; H, 3.59%. $Ni^{II}_{1.5}[Cr^{III}(CN)_6]\cdot 8.0H_2O$ (**NiCr**)**,** Calculated: Ni, 20.00; Cr, 11.81; C, 16.37; N, 19.09; H, 3.66%; Found: Ni, 19.96; Cr, 11.94; C, 16.50; N, 19.35; H, 3.39%. $K^{I}_{0.16}Mn^{II}_{1.42}[Co^{III}(CN)_6]\cdot 5.8H_2O$ (**MnCo**), Calculated: K, 0.78; Mn, 19.91; Co, 14.63; C, 17.89; N, 20.86; H, 3.66%; Found: K, 0.84; Mn, 19.95; Co, 15.01; C, 17.76; N, 20.55; H, 3.66%. $Fe^{II}_{1.55}[Co^{III}(CN)_6]_{0.9}[Co^{II}(CN)_6]_{0.1}\cdot 7.7H_2O$ (**FeCo**), Calculated: Fe, 19.66; Co, 13.38; C, 16.36; N, 19.09; H, 3.52%; Found: Fe, 19.41; Co, 13.05; C, 16.64; N, 19.15; H, 3.23%. $Co^{II}_{1.5}[Co^{III}(CN)_6]\cdot 7.5H_2O$ (**CoCo**), Calculated: Co^{II}, 20.16; Co^{III}, 13.44; C, 16.43; N, 19.17; H, 3.45%; Found: Co^{II}, 20.36; Co^{III}, 13.57; C, 16.41; N, 18.81; H, 3.34%. $Ni^{II}_{1.5}[Co^{III}(CN)_6]\cdot 8.9H_2O$ (**NiCo**), Calculated: Ni, 19.00; Co, 12.72; C, 15.55; N, 18.14; H, 3.87%; Found: Ni, 18.92; Co, 12.84; C, 15.59; N, 17.86; H, 3.48%. $Cu^{II}_{1.55}[Co^{III}(CN)_6]_{0.9}[Co^{II}(CN)_6]_{0.1}\cdot 7.0H_2O$ (**CuCo**), Calculated: Cu, 22.40; Co, 13.40; C, 16.38; N, 19.12; H, 3.20%; Found: Cu, 22.56; Co, 13.19; C, 16.60; N, 19.11; H, 3.04%.

The IR spectra of these nine samples were recorded before and after the application of pressure to assess the change in the intensity of the IR peak of water (Figure S6, Tables S3 and S4). The intensity of this peak of the CuCr PBA decreased the most with pressure application. These results suggest that higher water content in the samples does not necessarily correlate with an increase in water production with pressure. Additionally, when the cyanide center metal was $Co(CN)_6$, the IR spectra recorded before and after the application of pressure only differed slightly. In contrast, when the cyanide center metal was $Cr(CN)_6$, except for **MnCr**, the IR peak intensity of water decreased upon the application of pressure. This observation suggests that, for water production under pressure, the cyanide-center metal should be $Cr(CN)_6$ rather than $Co(CN)_6$. Furthermore, the XRD pattern of each sample was acquired before and after the application of pressure, and analysed by Rietveld refinement. The results confirmed that the crystal frameworks were maintained in all samples after the application of pressure (Figures S7 and S8). In addition, the particle size of each sample was evaluated using SEM (Figure S9, Tables S3 and S4). These results suggest that the particle size is not correlated to the water production.

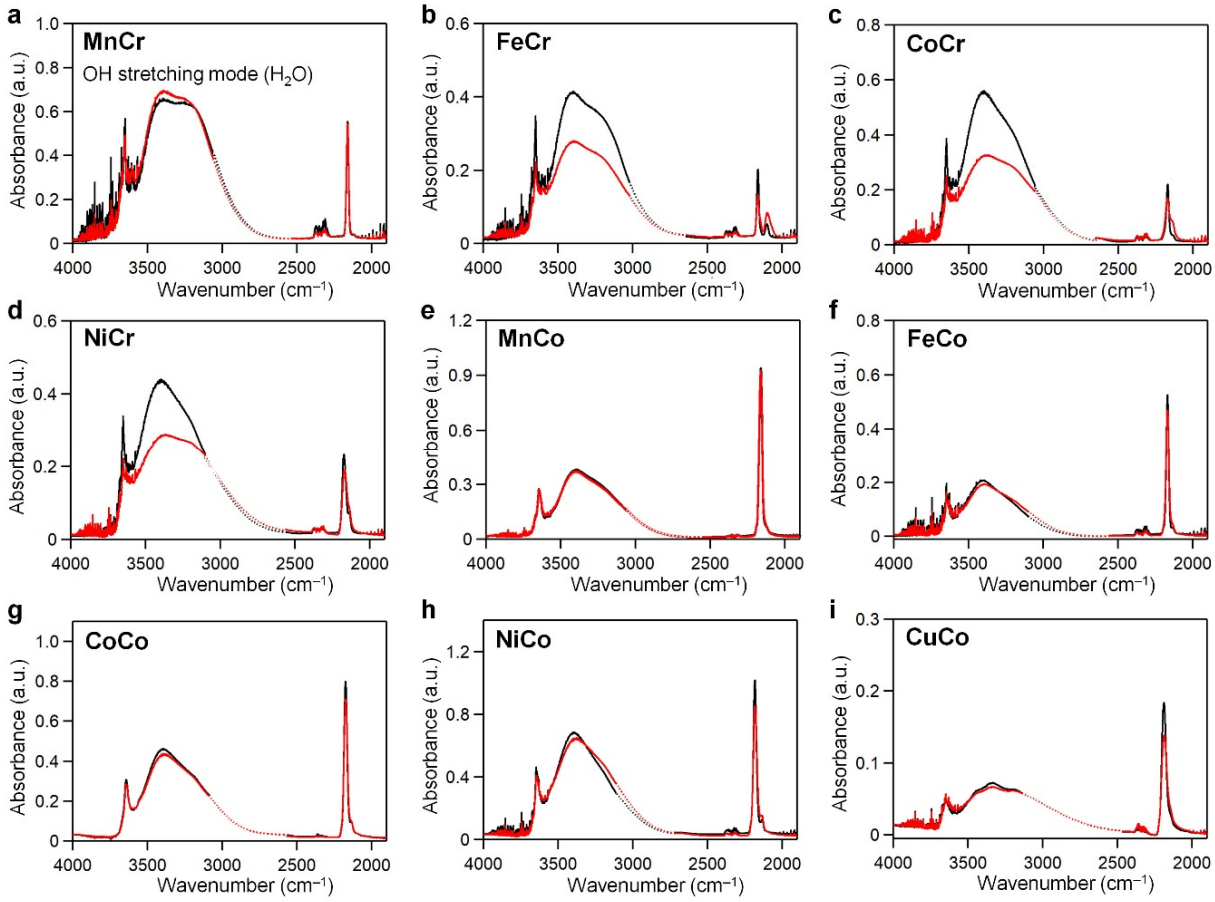

Figure S6. IR spectra before (black curve) and after (red curve) the application of 2 GPa pressure. The experimentally acquired spectra are shown as solid curves, and the extrapolated spectra, based on the sampling procedure outlined in §7 of the Supporting Information, are shown as dotted curves.

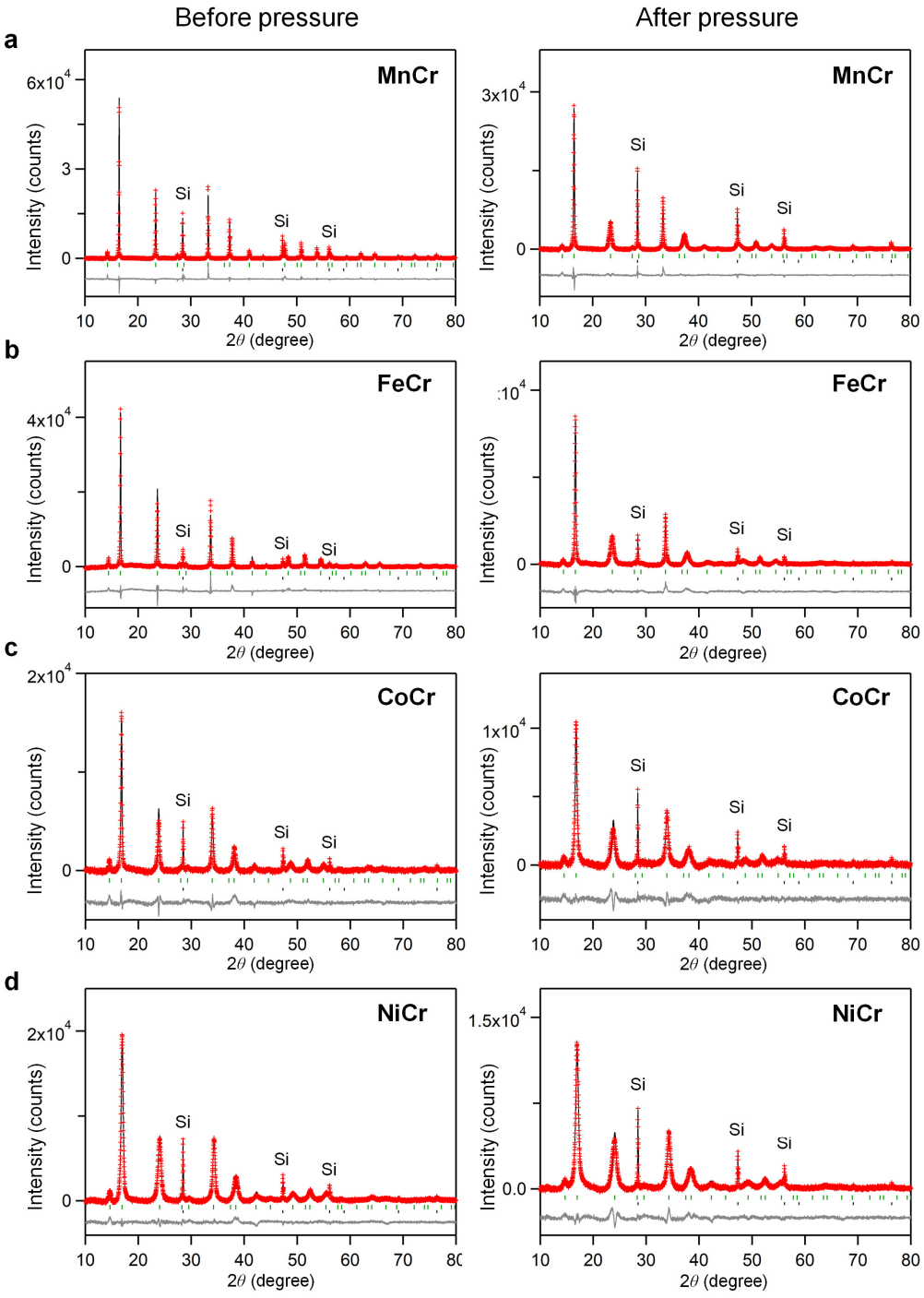

Figure S7. XRD patterns and Rietveld analyses of **MnCr** (a), **FeCr** (b), **CoCr** (c), and **NiCr** (d) PBAs before (left) and after (right) applying pressure of 2 GPa. The red dots, black lines, and grey lines represent the observed pattern, calculated pattern, and their difference, respectively. The green and black bars indicate the calculated positions of the Bragg reflections for PBA and Si, respectively. Si powder was used as a standard sample to calibrate the XRD patterns. All crystal structures were cubic ($Fm\bar{3}m$), and the lattice constants obtained by Rietveld refinement of the XRD patterns (before pressure, after pressure) were (10.771 Å, 10.773 Å) for **MnCr**, (10.647 Å, 10.644 Å) for **FeCr**, (10.565 Å, 10.558 Å) for **CoCr**, and (10.460 Å, 10.455 Å) for **NiCr**.

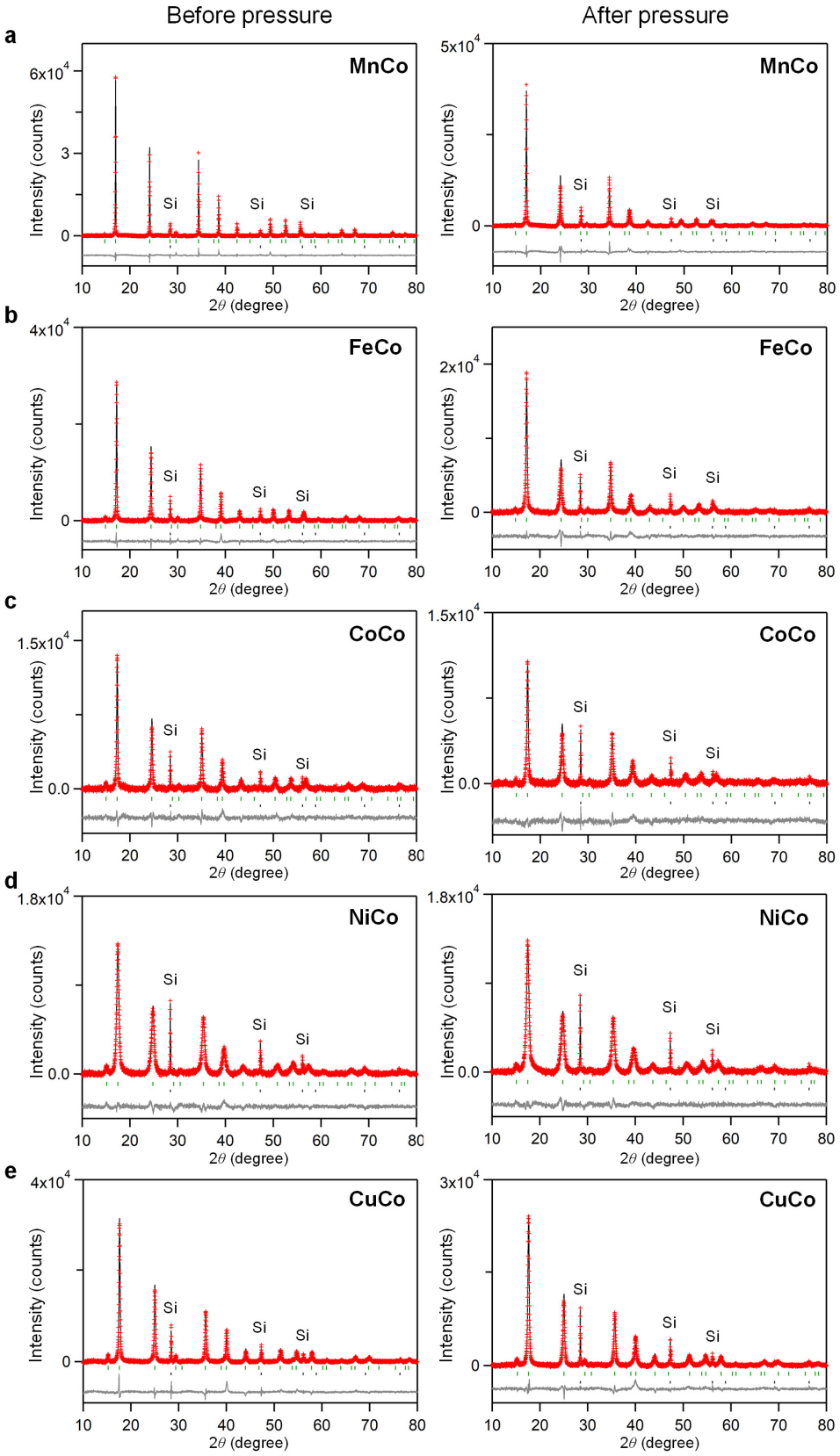

Figure S8. XRD patterns and Rietveld analyses of **MnCo** (a), **FeCo** (b), **CoCo** (c), **NiCo** (d), and **CuCo** (e) PBAs before (left) and after (right) applying pressure of 2 GPa. The red dots, black line, and grey line represent the observed pattern, calculated pattern, and their difference, respectively. The green and black bars indicate the calculated positions of the Bragg reflections for PBA and Si, respectively. Si powder was used as a standard sample to calibrate the XRD patterns. All crystal structures were cubic ($Fm\bar{3}m$), and the lattice constants obtained by Rietveld refinement of the XRD patterns (before pressure, after pressure) were (10.4346 Å, 10.432 Å) for **MnCo**, (10.647 Å, 10.644 Å) for **FeCo**, (10.309 Å, 10.311 Å) for **CoCo**, (10.239 Å, = 10.243 Å) for **NiCo**, and (10.148 Å, 10.153 Å) for **CuCo.**

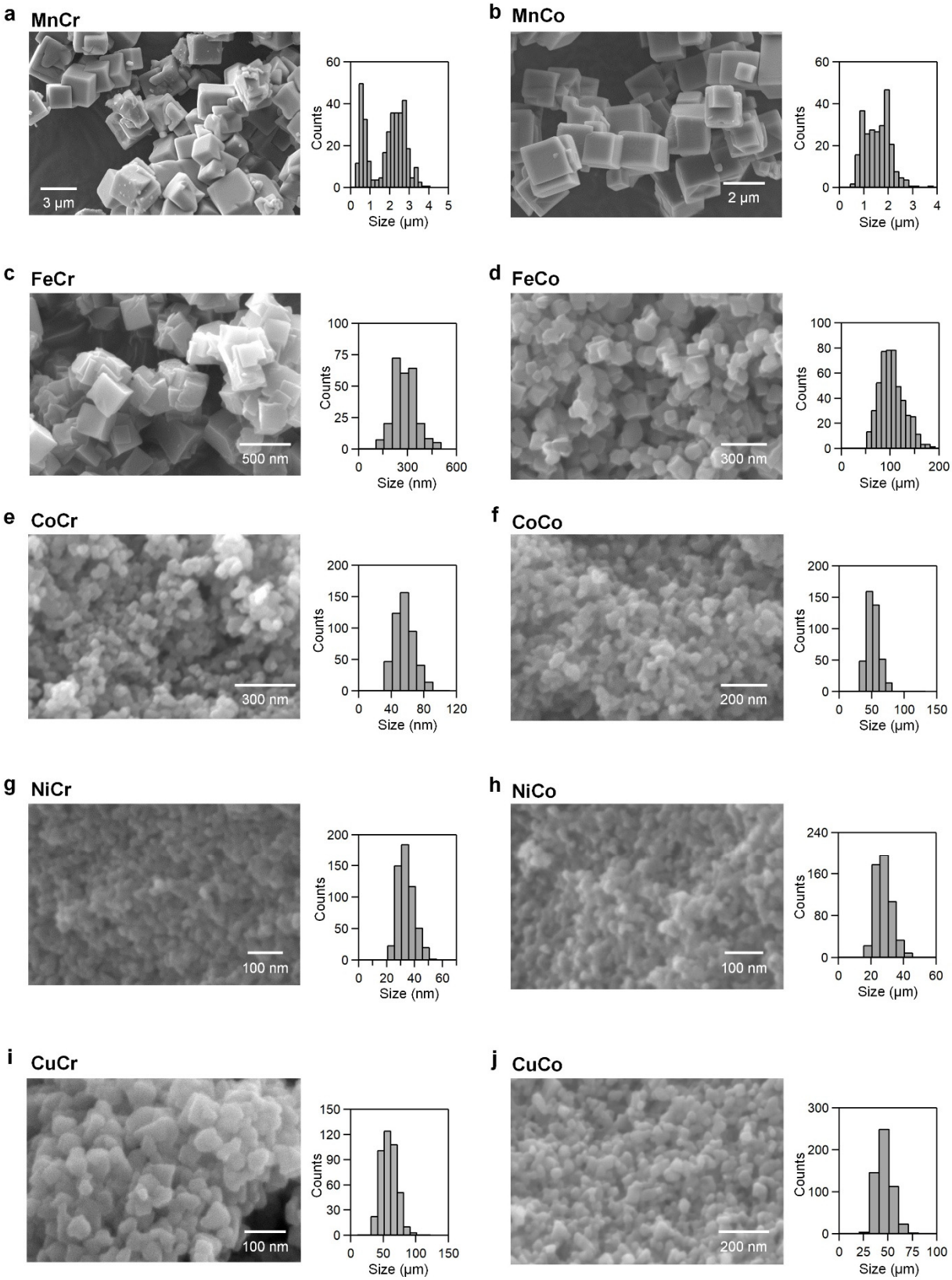

Figure S9. SEM images (left) and size distribution (right) for **MnCr** with 1.6 ± 0.9 μm (a), **MnCo** with 1.32 ± 0.53 μm (b), **FeCr** with 228 ± 70 nm (c), **FeCo** with 92 ± 26 nm (d), **CoCr** with 45 ± 12 nm (e), **CoCo** with 41 ± 11 nm (f), **NiCr** with 36 ± 17 nm (g), **NiCo** with 22 ± 5 nm (h), **CuCr** with 48 ± 12 nm (i), and **CuCo** with 36 ± 9 nm (j).

Table S3. Number of water (*z*) measured at 26 °C and 27% RH (top), change in the IR peak area of water upon pressure application (middle), and particle size estimated from the SEM image (bottom) in various PBAs of $M[Cr(CN)_6]\cdot zH_2O$ (*M* = Mn, Fe, Co, Ni, Cu).

Sample	**MnCr**	**FeCr**	**CoCr**	**NiCr**	**CuCr**
Number of water (*z*)	8.0	7.2	8.3	8.0	6.4
Change of IR peak area (%)	+0.5	−30.8	−28.6	−21.0	−33.9
Particle size	1.6 ± 0.9 μm	228 ± 70 nm	45 ± 12 nm	36 ± 17 nm	48 ± 12 nm

Table S4. Number of water (*z*) measured at 26 °C and 27% RH (top), change in the IR peak area of water upon pressure application (middle), and particle size estimated from the SEM image (bottom) in various PBAs of $M[Co(CN)_6]\cdot zH_2O$ (*M* = Mn, Fe, Co, Ni, Cu).

Sample	**MnCo**	**FeCo**	**CoCo**	**NiCo**	**CuCo**
Number of water (*z*)	5.8	7.7	7.5	8.9	7.0
Change of IR peak area (%)	−1.3	+1.2	−3.3	+2.1	−1.6
Particle size	1.32 ± 0.53 μm	92 ± 26 nm	41 ± 11 nm	22 ± 5 nm	36 ± 9 nm

§10. IR spectra of CuCr PBA after pressure application of 7.5 x 10^{-2} GPa for XES and XAS measurements.

The intensity changes observed in XES and XAS spectra for O 1s by pressure application are relatively small compared to that of IR spectra. One of the possible reasons is that the sample before applying pressure actually experiences a pressure of 7.5 x 10^{-2} GPa to form a pellet (Fig. S10).

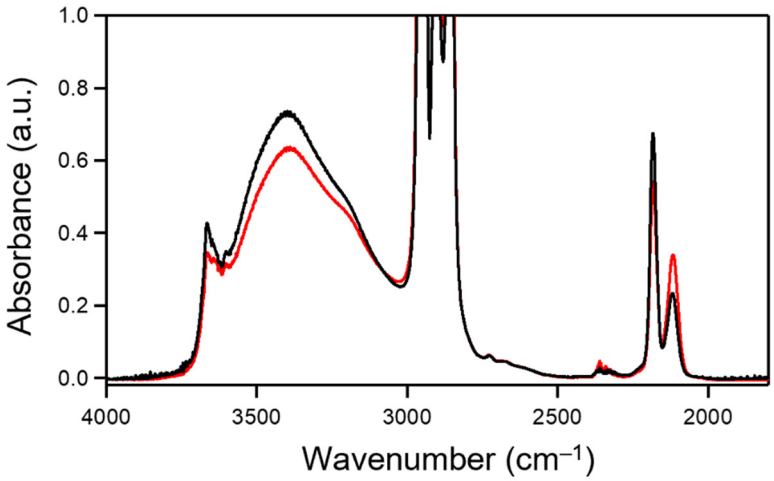

Figure S10. IR spectra of CuCr PBA as synthesized (black line) and after pressure application of 7.5 x 10^{-2} GPa (red line).

Author Contributions

S.A. and M.T. performed sample syntheses, characterizations, IR measurements, XRD measurements, TG measurements, pressure application experiments, and data analyses. J.W. contributed to the data analyses. H.K. and Y.H. conducted XES and XAS measurements using the Synchrotron Radiation system. Y.C. and K.M. discussed data interpretation and mechanisms. K.I. contributed to the sample syntheses, characterizations, and TG measurements. S.O. contributed to data analysis and interpretation of the mechanisms. H.T. designed and coordinated this study, contributed to all measurements and analyses, and wrote the paper. All authors contributed to the discussion and editing of the manuscript.